33rd Annual International Conference of the IEEE EMBS
Boston, Massachusetts USA, August 30 - September 3, 2011

Breath gas analysis for estimating physiological processes using anesthetic monitoring as a prototypic example

Julian King, Karl Unterkofler, Susanne Teschl, Anton Amann, and Gerald Teschl

Abstract— **Analysis of exhaled trace gases is a novel methodology for gaining continuous and non-invasive information on the clinical state of an individual. This paper serves to explore some potential applications of breath gas analysis in anesthesia, describing a monitoring scheme for target site concentrations and cardiac output via physiological modeling and *real-time* breath profiles of the anesthetic agent. The rationale given here is mainly simulation-based, however, the underlying concepts are directly applicable to a routine clinical setting.**

I. INTRODUCTION

Breath analysis is a relatively young field of research centering on the detection and quantification of volatile organic compounds (VOCs) appearing in human breath [1]. Such trace gases are either released endogenously or penetrate the body as a result of exogenous exposure, eventually entering the blood stream and being metabolized or excreted via exhalation, skin emission, urine, etc.. Exhaled breath analysis employed for medical testing/diagnosis and monitoring has the advantage of being *non-invasive*. Breath samples can be extracted as often as desired and can be measured in *real-time* as well as with breath-by-breath resolution, e.g., by using proton-transfer-reaction mass spectrometry (PTR–MS) [2]. Breath analysis hence is an optimal choice for gaining *continuous* information on the physiological state of an individual, even under challenging conditions, e.g., during operations or at an intensive care unit. Within this context, the present paper serves to explore some potential applications of breath gas analysis in anesthesia. Due to the current lack of appropriate *in vivo* data the rationale given here is mainly simulation-based, however, the underlying concepts are directly applicable to a routine clinical setting.

A core task in anesthesia is to control anesthetic depth by administering adequate amounts of the anesthetic agent to the target (effect) sites in the central nervous system (CNS). While a well-defined relationship between target site concentrations (TSCs) and the associated anesthetic/amnestic response can be expected, assessments of the latter usually rest on derivational variables that can relatively easily be accessed by direct measurement. In inhalation anesthesia, a quantity of considerable interest is the minimum alveolar concentration (MAC), defined as the end-tidal concentration of the agent at which 50% of the patients fail to respond to surgical incision. However, the MAC value is essentially a steady state concept. Indeed, during transient states following a modification of the inspired gas concentration (e.g., induction) the end-tidal agent concentration is a poor indicator for the TSC. A more reliable estimation of anesthetic CNS levels would hence be highly desirable [3]. Similarly, for intravenous drugs the respective serum level often serves as a surrogate for the underlying TSC. As has been suggested by several authors, the former might also be estimated via breath measurements, thus obviating the time-intensive analysis of blood samples. For perspective, a good agreement between breath propofol content (determined, e.g., by PTR–MS at $m/z = 179$) and serum levels has been reported [4].

A second hallmark of anesthesia is the need for continuous monitoring of vital respiratory and hemodynamic parameters. While ventilation is usually adjusted automatically by means of a breathing circuit (for ensuring stable normocapnic conditions), perfusion (i.e., cardiac output $\dot{Q}_{\mathrm{c}}$) is a rather intricate quantity to determine, particularly due to the inaccessibility of current stroke volumes. Reliable measurements of $\dot{Q}_{\mathrm{c}}$ are imperative for combating many circulatory complications, however, most of the conventional methods for pursuing this goal are either highly invasive (dye or thermal dilution) or cumbersome (ultrasonic techniques, impedance cardiography). Alternatively, it is well-known that $\dot{Q}_{\mathrm{c}}$ can also be reconstructed from the breath dynamics of exhaled inert gases (*Fick principle*), which is the approach that we shall adopt here. The inert gas employed will be the anesthetic agent itself, i.e., no additional instrumentation is involved.

Specifically, our goal is to describe a novel on-line monitoring scheme for $\dot{Q}_{\mathrm{c}}$ and the desired TSCs using physiological modeling and breath profiles of the anesthetic drug. Our account is strongly influenced by the earlier demonstration in [5], however, it differs from the latter by providing some model validation with clinical data and by using an estimation procedure fully exploiting the underlying model structure. The presentation in the sequel focuses on the prototypic volatile anesthetic sevoflurane, which is a convenient choice in terms of clinical relevance, measurability and availability of experimental data [6]. Particularly, this agent can be detected in PTR–MS at $m/z = 181$ [7], thus allowing for direct *real-time* measurements of the associated alveolar (end-tidal) concentrations. Sevoflurane is especially suitable for tracking hemodynamic/respiratory events due to the compound's low blood:gas partition coefficient $\lambda_{\mathrm{b:air}} = 0.6$ [8], implying a high sensitivity of the associated breath output with respect to blood and ventilatory flow.

J. King and G. Teschl are with the Faculty of Mathematics, University of Vienna, A-1090 Wien, Austria (jking@oeaw.ac.at, gerald.teschl@univie.ac.at)

J. King, K. Unterkofler, and A. Amann are with the Breath Research Institute of the Austrian Academy of Sciences, A-6850 Dornbirn, Austria (ku@fhv.at, anton.amann@oeaw.ac.at)

S. Teschl is with the University of Applied Sciences Technikum Wien, A-1200 Wien, Austria (susanne.teschl@esi.ac.at)

II. SIMULATION AND ESTIMATION

A. Physiological model

The usual compartmental approach is adopted for capturing the tissue accumulation of sevoflurane during inhalation anesthesia. The systemic part of the model is similar to previously developed physiologically based descriptions of sevoflurane pharmacokinetics [3] and incorporates three well-mixed functional units: brain tissue (target site), a richly perfused tissue (RPT) compartment (liver, kidneys, muscle), lumping together tissue groups with comparable blood:tissue partition coefficient $\lambda_{\mathrm{b:rpt}} \approx 0.24$ [8], as well as a buffer tissue (fat), acting as a reservoir for the lipophilic agent sevoflurane. All three compartments receive a *constant* share of $\dot{Q}_{\mathrm{c}}$ and are separated into the intracellular space and the vascular blood, whereby a venous equilibrium holds at these interfaces. It is postulated that the major route of sevoflurane uptake and removal is respiration, governed by the alveolar ventilation $\dot{V}_{\mathrm{A}}$. In particular, metabolic clearance is assumed to be negligible [6]. The lung is modeled by one single homogenous alveolar unit characterized by an average ventilation-perfusion ratio close to one in normal healthy patients at rest. Since both venous admixture and physiological dead space are higher during general anesthesia than in the awake state, a constant shunt fraction $q_{\mathrm{s}} = 0.1$ and an alveolar dead space fraction $v_{\mathrm{ad}} = 0.1$ are incorporated into the model [9]. Pulmonary gas exchange is assumed to be perfusion-limited, i.e., an instantaneous equilibrium is established between the end-capillary concentrations $C_{\mathrm{c}'}$ and alveolar levels C_{A}, viz., $C_{\mathrm{c}'} = C_{\mathrm{A}}\lambda_{\mathrm{b:air}}$. The model structure is presented in Fig. 1. For a detailed nomenclature we refer to Table I.

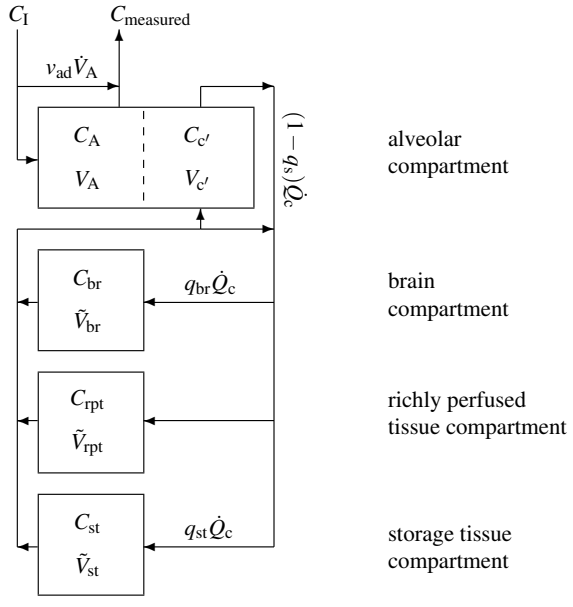

Fig. 1. Sketch of the sevoflurane model structure. The body is divided into four distinct functional units: alveolar/end-capillary compartment (gas exchange), brain tissue (effect site), richly perfused tissue and storage tissue (adipose tissue). Dashed boundaries indicate a diffusion equilibrium.

From the previous assumptions the mass balance equation for the alveolar compartment reads

$$\tilde{V}_{\mathrm{A}}\frac{\mathrm{d}C_{\mathrm{A}}}{\mathrm{d}t} = (1-v_{\mathrm{ad}})\dot{V}_{\mathrm{A}}(C_{\mathrm{I}} - C_{\mathrm{A}}) + (1-q_{\mathrm{s}})\dot{Q}_{\mathrm{c}}(C_{\bar{\mathrm{v}}} - C_{\mathrm{A}}\lambda_{\mathrm{b:air}}), \quad (1)$$

where C_{I} denotes the inhaled sevoflurane concentration and $\tilde{V}_{\mathrm{A}} = V_{\mathrm{A}} + \lambda_{\mathrm{b:air}}V_{\mathrm{c}'}$ is the *effective* alveolar volume taking into account the amount of sevoflurane dissolved in capillary blood. Similarly, for the brain, richly perfused and storage tissue compartment we find that

$$\tilde{V}_{\mathrm{br}}\frac{\mathrm{d}C_{\mathrm{br}}}{\mathrm{d}t} = q_{\mathrm{br}}\dot{Q}_{\mathrm{c}}(C_{\mathrm{a}} - \lambda_{\mathrm{b:br}}C_{\mathrm{br}}), \quad (2)$$

and

$$\tilde{V}_{\mathrm{rpt}}\frac{\mathrm{d}C_{\mathrm{rpt}}}{\mathrm{d}t} = (1-q_{\mathrm{br}}-q_{\mathrm{st}})\dot{Q}_{\mathrm{c}}(C_{\mathrm{a}} - \lambda_{\mathrm{b:rpt}}C_{\mathrm{rpt}}), \quad (3)$$

and

$$\tilde{V}_{\mathrm{st}}\frac{\mathrm{d}C_{\mathrm{st}}}{\mathrm{d}t} = q_{\mathrm{st}}\dot{Q}_{\mathrm{c}}(C_{\mathrm{a}} - \lambda_{\mathrm{b:st}}C_{\mathrm{st}}), \quad (4)$$

respectively. Here, the associated concentrations in mixed venous and arterial blood are given by the weighted means

$$C_{\bar{\mathrm{v}}} := q_{\mathrm{br}}\lambda_{\mathrm{b:br}}C_{\mathrm{br}} + (1-q_{\mathrm{br}}-q_{\mathrm{st}})\lambda_{\mathrm{b:rpt}}C_{\mathrm{rpt}} + q_{\mathrm{st}}\lambda_{\mathrm{b:st}}C_{\mathrm{st}} \quad (5)$$

and

$$C_{\mathrm{a}} := (1-q_{\mathrm{s}})C_{\mathrm{A}}\lambda_{\mathrm{b:air}} + q_{\mathrm{s}}C_{\bar{\mathrm{v}}}, \quad (6)$$

respectively. Moreover, the measured (*end-tidal*) sevoflurane concentration equals

$$C_{\mathrm{measured}} = (1-v_{\mathrm{ad}})C_{\mathrm{A}} + v_{\mathrm{ad}}C_{\mathrm{I}}. \quad (7)$$

The clinical adequacy of the above formulation was tested by comparing the resulting model predictions to an ensemble of *in vivo* concentration profiles published in [3]. By adopting the reference values in Table I and setting the initial concentration of each compartment to zero, the simulated model dynamics are in good agreement with the observed data, see Fig. 2.

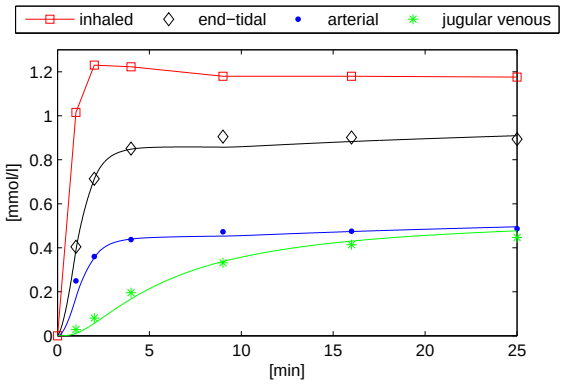

Fig. 2. Simulation of sevoflurane profiles in inspired air (C_{I}), end-tidal air (C_{measured}, cf. (7)), arterial blood (C_{a}, cf. (6)), and jugular venous blood (corresponding to $C_{\mathrm{br}}\lambda_{\mathrm{b:br}}$) during administration of approx. 3% sevoflurane over 25 min. Discrete points reflect sample means associated with *pooled* data from 11 patients as measured in [3].

Note that during anesthesia induction the end-tidal sevoflurane profile yields a poor representation of the underlying TSC dynamics. Specifically, while the former readily approaches the desired MAC of about 2%, jugular venous blood levels are still in a transitory phase.

B. Anesthetic monitoring: a proof of concept

As has been pointed out in the introduction, the variables C_{I} and C_{A} can be viewed as known or measurable quantities within a routine setting, while $\dot{Q}_{\mathrm{c}}$ will be interpreted as an additional time-varying parameter θ that has to be estimated from the available breath sevoflurane data. Its time evolution will be modeled as a random walk. By employing zero-order hold sampling and introducing process as well as measurement noise, (1)–(7) can straightforwardly be transformed into a discrete time-varying stochastic system of the form

$$\begin{aligned} \mathbf{x}_k &= G_{k-1}(\theta_{k-1})\mathbf{x}_{k-1} + \mathbf{f}_{k-1} + \mathbf{w}_{k-1} \\ \theta_k &= \theta_{k-1} + \vartheta_{k-1} \\ y_k &= H_k\mathbf{x}_k + d_k + v_k, \end{aligned} \tag{8}$$

in the state variable $\mathbf{x} := \begin{pmatrix} C_{\mathrm{A}} & C_{\mathrm{br}} & C_{\mathrm{rpt}} & C_{\mathrm{st}} \end{pmatrix}^T$, with the scalar output being given by $y_k := C_{\mathrm{measured},k}$. Here, the postulated sampling interval is 5 s, roughly corresponding to the duration of one respiratory cycle during normal breathing at 12 tides/min. We assume that $\{\mathbf{w}_k\}$, $\{\vartheta_k\}$, and $\{v_k\}$ can be simulated as Gaussian, white, zero-mean noise sequences with known covariance matrices Q_k, T_k, and R_k, respectively. Additionally, we assign the Gaussian prior densities

$$p(\mathbf{x}_0) \sim \mathcal{N}(\mathbf{0}, \mathrm{O}), \quad p(\theta_0) \sim \mathcal{N}(\dot{Q}_{\mathrm{c}}^{\mathrm{est}}, \mathrm{var}\{\dot{Q}_{\mathrm{c}}^{\mathrm{est}}\}), \tag{9}$$

encapsulating our information on the initial sevoflurane concentrations as well as on the initial cardiac output. Here, O denotes the zero matrix of appropriate size.

Using the representation in (8) we may directly aim at the joint estimation of $\mathbf{x}$ and θ from the observable profile of the breath sevoflurane concentration y by virtue of *Bayesian filtering* methods as illustrated below. Due to the lack of appropriate *in vivo* data, a sequence of data points $\mathbf{x}_k$ is *simulated* from the undisturbed system by employing predefined profiles for $\dot{Q}_{\mathrm{c}}$, $\dot{V}_{\mathrm{A}}$, and C_{I} (cf. Fig. 3), setting $\mathbf{x}_0 = \mathbf{0}$ (i.e., we assume that no sevoflurane is present in the body at the onset of anesthesia). Subsequently, noisy output data y_k are created from (8) by applying additive Gaussian perturbations with fixed variance $R_k = (0.008)^2$.

Sequential state and parameter reconstruction from the stacked observations $Y_k := (y_k, \ldots, y_1)$ can be achieved by virtue of a marginalized particle filtering scheme as introduced in [10]. Briefly, the central object of interest within this framework is the conditional (*posterior*) probability $p(\mathbf{x}_k, \Theta_k|Y_k)$, which embodies all accessible information on $\mathbf{x}_k$ and the parameter sequence $\Theta_k := (\theta_k, \ldots, \theta_0)$ up to time k. For the purpose of computing this density, it is instructive to note that, conditional on Θ_k, (8) represents a linear Gaussian system, i.e., we may decompose

$$p(\mathbf{x}_k, \Theta_k|Y_k) = p(\mathbf{x}_k|\Theta_k, Y_k)p(\Theta_k|Y_k), \tag{10}$$

where the first factor $p(\mathbf{x}_k|\Theta_k, Y_k) \sim \mathcal{N}(\hat{\mathbf{x}}_k^+(\Theta_k), P_k^+(\Theta_k))$ can be determined analytically by means of the standard Kalman filter formulae. As for the second factor, using *Bayes' Theorem* and taking into account the specific structure of (8) one finds the recursion

$$\begin{aligned} p(\Theta_k|Y_k) = \frac{p(y_k|\theta_k, Y_{k-1})}{p(y_k|Y_{k-1})} p(\theta_k|\Theta_{k-1}, Y_{k-1}) \times \\ p(\Theta_{k-1}|Y_{k-1}). \end{aligned} \tag{11}$$

The goal of particle filtering is to approximate this density by drawing $m \gg 1$ random samples $\{\Theta_{k,1}^+, \ldots, \Theta_{k,m}^+\}$ from it, producing a point mass representation of the form $p(\Theta_k|Y_k) \cong m^{-1}\sum_j \delta_{\Theta_{k,j}^+}(\Theta_k)$. Here, δ denotes the Dirac delta point measure. Plugging this expression into (10) one may directly compute estimators of the form

$$\begin{aligned} E\{\phi(\mathbf{x}_k, \Theta_k)|Y_k\} &= \int \phi(\mathbf{x}_k, \Theta_k) p(\mathbf{x}_k, \Theta_k|Y_k) \mathrm{d}\Theta_k \mathrm{d}\mathbf{x}_k \\ &\cong \frac{1}{m}\sum_{j=1}^{m} E\{\phi(\mathbf{x}_k, \Theta_{k,j}^+)|\Theta_{k,j}^+, Y_k\}. \end{aligned}$$

In the specific situation above, by setting $\phi(\mathbf{x}_k, \Theta_k) = \mathbf{x}_k$ we arrive at the MMSE estimate

$$E\{\mathbf{x}_k|Y_k\} \cong \frac{1}{m}\sum_{j=1}^{m} \hat{\mathbf{x}}_k^+(\Theta_{k,j}^+), \tag{12}$$

and similarly for $\phi(\mathbf{x}_k, \Theta_k) = \theta_k$. From (11), by adopting the standard *sampling importance resampling* scheme [11] the particle trajectories $\Theta_{k,j}^+$ can be updated as follows:

1) Invoke Kalman filtering to obtain the *a priori* state estimates $\hat{\mathbf{x}}_k^-(\theta_{k-1,j}^+)$ as well as $P_k^-(\theta_{k-1,j}^+)$ and propagate $\theta_{k-1,j}^+$ through the system dynamics (8) to arrive at *a priori* particles $\theta_{k,j}^-$.
2) Use y_k to compute the likelihoods $p(y_k|\theta_{k,j}^-, Y_{k-1}) \sim \mathcal{N}(H_k\hat{\mathbf{x}}_k^-(\theta_{k-1,j}^+) + d_k, H_k P_k^-(\theta_{k-1,j}^+)H_k^T + R_k)$.
3) Resample $\theta_{k,j}^+$ according to a multinomial distribution $\{(\theta_{k,1}^-, q_1), \ldots, (\theta_{k,m}^-, q_m)\}$ with the normalized likelihoods $q_j = p(y_k|\theta_{k,j}^-, Y_{k-1}) / \sum_j p(y_k|\theta_{k,j}^-, Y_{k-1})$.

In a final step, the new *a posteriori* particles $\theta_{k,j}^+$ are used in the measurement update of the corresponding Kalman filter. Summarizing, marginalized particle filtering for *joint* state and parameter estimation in models of the form (8) essentially incorporates running a bank of m separate Kalman filters in parallel (each one being associated with a single particle trajectory $\Theta_{k,j}$) and combining them like in (12).

The applicability of this filtering scheme within the anesthetic monitoring framework introduced above is demonstrated in Fig. 3. Here, the parameters of the prior density $p(\theta_0)$ in (9) were defined as $\dot{Q}_{\mathrm{c}}^{\mathrm{est}} = 8$ l/min and $\mathrm{var}\{\dot{Q}_{\mathrm{c}}^{\mathrm{est}}\} = (3)^2$. Following common practice, the process noise covariance matrices Q_k and T_k were tuned to ensure a satisfactory performance of the algorithm. In particular we set $T_k = (0.3)^2$ as a tradeoff between short transition times (for tracking, e.g., a step change in perfusion) and estimation accuracy.

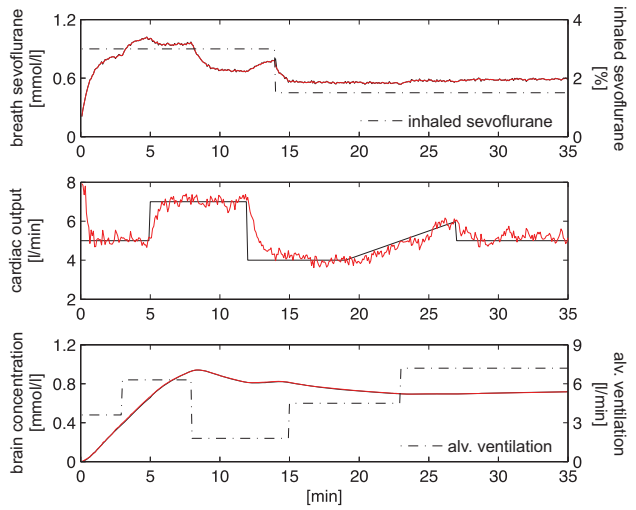

Fig. 3. Simulated (solid black) and recovered (solid red, almost overlapping) profiles of the breath sevoflurane concentration C_{measured}, cardiac output $\dot{Q}_{\mathrm{c}}$ and brain concentration C_{br}, using a marginalized particle filter with cloud size $m = 300$. Dash-dotted lines represent the profiles of C_{I} and $\dot{V}_{\mathrm{A}}$ used for the simulation of breath sevoflurane data.

The state and parameter estimates calculated from (12) faithfully reproduce their simulated counterparts. In particular, incidences such as abrupt drops in cardiac output appear to be trackable within a delay time that is adequate for enabling intra-operative interventions.

III. CONCLUSIONS AND FUTURE WORK

While we believe that the present approach can potentially contribute to facilitating *real-time* assessments of the anesthetic state on the basis of exhaled breath measurements, several aspects have to be investigated more deeply before this method can become clinically relevant, e.g., as a part of automated anesthesia delivery systems. A primary building block is the availability of a reliable physiological model for the endogenous concentration profiles of the inhalational/intravenous agent under study. Consequently, additional experimental efforts, data gathering and modeling attempts (accounting for substance-specific confounding factors, e.g., the redistribution of regional blood flow or possible metabolization/sequestration patterns in the pulmonary tract as in the case of propofol) are required in order to extend the validity of simple models such as the one presented above over a sufficiently wide range of possible dynamics. Moreover, further insights into the quantitative links between anesthetic depth and TSCs need to be gained.

In this sense, the previous analysis should mainly be seen as a proof of concept, coupling the high-frequency information obtainable from breath gas analytical techniques with well-established tools from signal processing in order to achieve a continuous monitoring of physiological processes.

IV. ACKNOWLEDGMENTS

The authors gratefully acknowledge support from the Austrian Science Fund (FWF) under Grant No. Y330 and the government of Vorarlberg, Austria.

TABLE I

BASIC MODEL PARAMETERS AND REFERENCE VALUES, CF. [12].

Parameter	Symbol	Nominal value [units]
Concentrations		
Alveoli	C_{A}	[mmol/l]
End-capillary	$C_{c'}$	
Inhaled	C_{I}	
Arterial	C_{a}	
Mixed-venous	$C_{\bar{\mathrm{v}}}$	
Brain tissue	C_{br}	
RPT (viscera, muscles)	C_{rpt}	
Storage tissue (fat)	C_{st}	
Compartment volumes		
Alveoli	V_{A}	4.1 [l]
End-capillary	$V_{c'}$	0.15 [l]
Brain	V_{br}	1.3 [l]
RPT (viscera, muscles)	V_{rpt}	40 [l]
Storage (fat tissue)	V_{st}	15 [l]
Flows		
Cardiac output	$\dot{Q}_{\mathrm{c}}$	4 [l/min]
Alv. ventilation	$\dot{V}_{\mathrm{A}}$	4 [l/min]
Fractional flow brain	q_{br}	0.135
Fractional flow storage	q_{st}	0.06
Shunt fraction	q_{s}	0.1
Alv. dead space fraction	v_{ad}	0.1
Partition coefficients		
Blood:air	$\lambda_{\mathrm{b:air}}$	0.6
Blood:brain	$\lambda_{\mathrm{b:br}}$	0.46
Blood:rpt	$\lambda_{\mathrm{b:rpt}}$	0.24
Blood:storage tissue	$\lambda_{\mathrm{b:st}}$	0.014

REFERENCES

[1] A. Amann and D. Smith, Eds., *Breath Analysis for Clinical Diagnosis and Therapeutic Monitoring*. Singapore: World Scientific, 2005.

[2] J. King, A. Kupferthaler, K. Unterkofler, H. Koc, S. Teschl, G. Teschl, W. Miekisch, J. Schubert, H. Hinterhuber, and A. Amann, "Isoprene and acetone concentration profiles during exercise on an ergometer," *J. Breath Res.*, vol. 3, p. 027006 (16pp), 2009.

[3] M. Nakamura, Y. Sanjo, and K. Ikeda, "Predicted sevoflurane partial pressure in the brain with an uptake and distribution model comparison with the measured value in internal jugular vein blood," *J. Clin. Monit. Comput.*, vol. 15, pp. 299–305, 1999.

[4] A. Takita, K. Masui, and T. Kazama, "On-line monitoring of end-tidal propofol concentration in anesthetized patients," *Anesthesiology*, vol. 106, pp. 659–664, 2007.

[5] O. Brovko, D. M. Wiberg, L. Arena, and J. W. Bellville, "The extended Kalman filter as a pulmonary blood flow estimator," *Automatica*, vol. 17, pp. 213–220, 1981.

[6] S. S. Patel and K. L. Goa, "Sevoflurane. A review of its pharmacodynamic and pharmacokinetic properties and its clinical use in general anaesthesia," *Drugs*, vol. 51, pp. 658–700, 1996.

[7] G. Summer, P. Lirk, K. Hoerauf, U. Riccabona, F. Bodrogi, H. Raifer, M. Deibl, J. Rieder, and W. Schobersberger, "Sevoflurane in exhaled air of operating room personnel," *Anesth. Analg.*, vol. 97, pp. 1070–1073, 2003.

[8] V. Fiserova-Bergerova and M. L. Diaz, "Determination and prediction of tissue-gas partition coefficients," *Int. Arch. Occup. Environ. Health*, vol. 58, pp. 75–87, 1986.

[9] A. B. Lumb, *Nunn's Applied Respiratory Physiology*, 6th ed. Oxford: Butterworth-Heinemann, 2005.

[10] T. Schön, F. Gustafsson, and P.-J. Nordlund, "Marginalized particle filters for mixed linear/nonlinear state-space models," *IEEE Trans. Signal Processing*, vol. 53, pp. 2279–2289, 2005.

[11] N. J. Gordon, D. J. Salmond, and A. F. M. Smith, "A novel approach to nonlinear/non-Gaussian Bayesian state estimation," *IEE Proceedings F*, vol. 140, pp. 107–113, 1993.

[12] J. King, "Mathematical modeling of blood-gas kinetics for the volatile organic compounds isoprene and acetone," Ph.D. dissertation, Leopold-Franzens-Universität Innsbruck, 2010.